Hindawi Publishing Corporation
Journal of Sensors
Volume 2011, Article ID 608157, 9 pages
doi:10.1155/2011/608157

Research Article

Dark Signal Temperature Dependence Correction Method for Miniature Spectrometer Modules

Joel Kuusk

Group of Remote Sensing of Vegetation, Department of Atmospheric Physics, Tartu Observatory, 61602 Tõravere, Estonia

Correspondence should be addressed to Joel Kuusk, joel@scorpion.aai.ee

Received 27 September 2010; Revised 17 January 2011; Accepted 9 February 2011

Academic Editor: Amine Bermak

A dark signal temperature dependence correction method for miniature spectrometer modules is described in this paper. It is based on laboratory measurements of dark signal temperature dependence at few different integration times. A set of parameters are calculated which make it possible to estimate dark signal at any temperature and integration time within reasonable range. In field conditions, it is not always possible to take frequent dark signal readings during spectral measurements. If temperature is recorded during the measurement, this method can be used for estimating dark signal for every single spectral measurement. The method is validated on two different miniature spectrometers.

1. Introduction

Miniature spectrometer modules are becoming increasingly available. They provide a cost-effective way for designing small and lightweight spectrometer systems.

There are several possible fields of use for miniature spectrometer modules, for example, agriculture [1, 2], food industry [3, 4], health care [5], augmented sensory systems [6], and remote sensing [7–9]. Miniature spectrometer modules are most advantageous in those applications where essential demands to the measurement system include autonomy, ruggedness, small size, low weight, and/or limited power consumption. However, the same demands usually limit the possibilities of keeping the instruments at stable environmental conditions or taking frequent dark signal readings.

Dark signal is an inherent property of a spectrometer. It is the output signal of the spectrometer when the optical entrance is closed. During a target measurement, the output signal is the sum of the target signal and the dark signal. For extracting target signal, therefore, a precise knowledge of the dark signal is necessary. It is most important in spectral bands where measured signal is low either because of weak optical signal or low sensitivity of the sensor array.

Dark signal of a spectrometer is mainly the sum of two components. One is caused by the dark current, I_{dark}, of the detector element, which depends on the detector's temperature. In the case of junction-based detectors, it can be described with the following equation:

$$I_{\text{dark}} = I_0\left[\exp\left(\frac{qV}{kT}\right) - 1\right], \tag{1}$$

where q is elementary charge, V is bias voltage of the photodiode, k is the Boltzmann constant, T is absolute temperature, and I_0 is the reverse saturation current characteristic of the diode. The reverse saturation current is a strong function of temperature, and for silicon P-N junctions, for example, I_0 approximately doubles for each temperature increase of 10 K [10]. During the integration time, the dark current from the detector is integrated and gathered charge is proportional to the output signal. The other part of the dark signal is an offset that is added in an amplifier circuit and does not depend on temperature if the amplifier is of good quality. This part of the signal does not depend on integration time either.

Two airborne spectrometer systems UAVSpec2 and UAVSpec4SWIR have been designed in Tartu Observatory [11]. UAVSpec2 is based on the MMS-1 and UAVSpec4SWIR is based on the NIR-PGS-1.7 spectrometer modules manufactured by Carl Zeiss Jena GmbH. They have been used onboard a Robinson R22 helicopter for vegetation remote

Table 1: Parameters of the devices under test.

Module	MMS-1	NIR-PGS-1.7	NIR-PGS-2.2
Serial number	028582	047934	046973
Sensor type	NIR-enhanced Si	InGaAs	Long wavelength type InGaAs
Spectral range, nm	400–1100	960–1690	1000–2170
Sensor cooling	None	1-stage TE	2-stage TE
Temperature controller	None	PELTIER-tc	PELTIER-tc
Compatible FEE	FEE-HS	FEE-1M	FEE-1M

sensing [7, 8, 11], but both are small and light enough for being carried by an unmanned aerial vehicle (UAV). UAVSpecs are fully autonomous spectrometer systems and do not contain any moving parts except cooling fans. This makes them very rugged and especially suitable for a UAV carrier. However, this means that there are no optical shutters and dark signal measurements cannot be obtained during flight. The dark signal measured before and after the flight must be used. Since proper temperature stabilization would make the spectrometer systems too large and heavy for being carried by a UAV, it is necessary to know the exact relation between the dark signal and temperature in order to get reliable spectral measurements.

Three different miniature spectrometer modules manufactured by Carl Zeiss Jena GmbH are examined in this study. Those are a near infrared (NIR) enhanced version of MMS-1 with a spectral range of 400–1100 nm, NIR-PGS-1.7 with a spectral range of 960–1690 nm, and NIR-PGS-2.2 with a spectral range of 1000–2170 nm. Dark signal dependence on temperature and integration time is measured for all the spectrometers. A correction algorithm is developed, and it is validated on MMS-1 and NIR-PGS-1.7.

Big and expensive spectrometers usually come with built-in temperature corrections, but this information is often company business secret and it is not publicly available. So, it is not possible to directly compare the method described in this paper with previously used temperature correction methods. To the best of our knowledge, this is the first reported literature on the dark signal temperature dependence correction method for miniature spectrometer modules.

2. Method

2.1. Instrumentation. MMS-1 spectrometer module is built around a solid glass body. The imaging grating and 256-pixel Si linear array sensor are rigidly attached to the glass body. The spectrometer has a fiber optic input with cross-section converter—single fibers of the fiber bundle in linear configuration form the entrance slit [12]. The preamplifier, is also included in the spectrometer module. MMS-1 spectrometer module is equipped with a front end electronics (FEE) board FEE-HS manufactured by Tec5 AG. FEE generates the controlling signals for the photodiode array of the sensor module, preprocesses the analog video signal from the preamplifier and performs analog-to-digital conversion [13].

NIR-PGS-series modules have a collimator and focusing lens with a plane grating. Sensors are thermoelectrically (TE) cooled InGaAs linear arrays. NIR-PGS-1.7 uses a standard-type InGaAs sensor with 256 or 512 pixels. The one used in this study has a 256-pixel sensor array. NIR-PGS-2.2 is equipped with a long wavelength-type 256-pixel InGaAs detector. Fiber optic input is similar to the MMS-1 spectrometer module. NIR-PGS-series also have built-in preamplifiers [14, 15]. The spectrometer modules are equipped with FEE-1M boards. A PELTIER-tc temperature controller module manufactured by Tec5 AG is used for cooling of linear arrays of both NIR-PGS-series spectrometer modules. PELTIER-tc is a linear temperature controller module with proportional-integrational control (PI-control) which adjusts the current across the Peltier element to reach a sensor temperature equal to the preset setpoint temperature [16]. The sensor temperature is kept constant regardless of the ambient temperature.

Table 1 gives an overview of the parameters of all three spectrometer modules.

For each spectrometer, two external thermistors are used for temperature measurements. One is glued to the analog to digital converter (ADC) integrated circuit (IC) at FEE. Another thermistor measures the temperature of the sensor module. For MMS-1, it is attached to the body of the spectrometer module. For NIR-PGS-series, the thermistor is glued next to the operational amplifier and voltage reference ICs at the preamplifier board.

All the spectrometer modules are connected to a laptop or desktop personal computer (PC) via in-house designed microprocessor-controlled interface cards. The microprocessor controlles the integration time and handles the data transmission between the PC and FEE. It also measures supply voltage level and temperatures with its internal ADC. The acquisition software running on the PC is in-house designed as well.

2.2. Measurements. Dark signal temperature dependence at several different integration times was measured for all the spectrometers. A portable refrigerator which had both cooling and warming ability was used for controlling the ambient temperature. For each spectrometer, the temperature was recorded approximately once per second. Since the refrigerator did not have a temperature controller, it was not possible to measure dark signal after the stabilization of the temperature. Therefore, the measurements were made simultaneously with changing the temperature

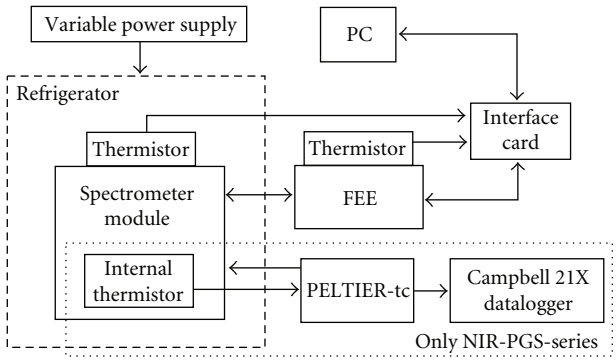

Figure 1: Experiment setup. The section inside dotted rectangle applies only to experiments with NIR-PGS-series spectrometer modules. The dashed rectangle represents the refrigerator.

and refrigerator supply voltage was adjusted to limit the temperature change rate. The maximum temperature change rate was 0.7°C /min and the average was 0.15–0.35°C/min for different spectrometers. Dark signal was measured at seven integration times: 120, 240, 480, 600, 1000, 2000, and 3000 ms. A script running on the PC looped through these settings and recorded 11–88 dark signal readings at every integration time. In addition, the sensor module and FEE were heated one at a time with a hot air gun to determine which part is more sensitive to temperature change.

For NIR-PGS-1.7 the Peltier current, setpoint voltage, and sensor temperature measured with the internal thermistor of the linear array were recorded from the PELTIER-tc temperature controller with a Campbell 21X datalogger. The experiment setup can be seen in Figure 1.

3. Results and Correction Algorithm

3.1. Dark Signal Temperature Dependence. Heating the spectrometer module and FEE separately revealed that dark signal depends significantly only on the temperature of the spectrometer module (see Figure 2). Both FEE-HS and FEE-1M showed similar behavior. Therefore, in this study only the temperatures recorded by the thermistor that was attached to the spectrometer module are used. In addition to measured temperature of the spectrometer module, effective temperature is plotted in Figure 2. This will be discussed in more detail in Section 3.2. Since only the temperature of the spectrometer module affected significantly the dark signal, it was the only component that was placed inside the refrigerator. This allowed to minimize the energy emitted inside the refrigerator and maximize the attainable temperature range.

In Figure 3, dark signal of a single band of MMS-1 with respect to the effective sensor temperature can be seen. Each group of points represent a different integration time. Since MMS-1 has an uncooled silicon sensor, its dark signal varies exponentially with temperature and linearly with integration time.

The dark signal temperature dependence of NIR-PGS-1.7 is shown in Figure 4. Its behavior is different compared to that of MMS-1. At shorter integration times, the relation

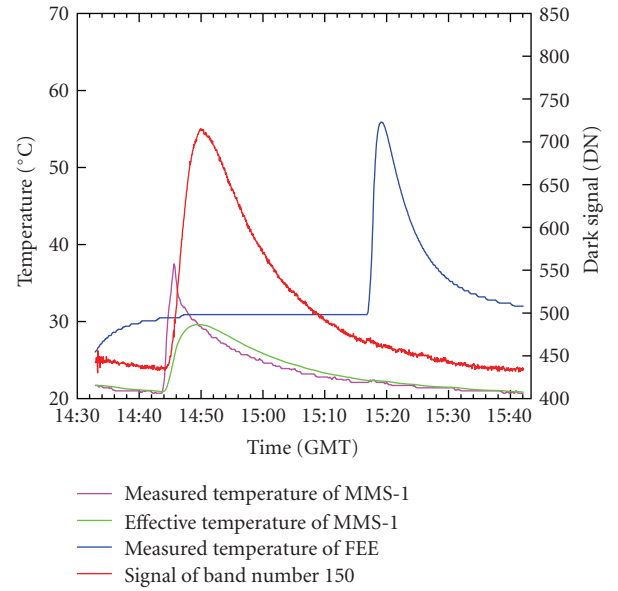

Figure 2: Dark signal during heating of MMS-1 and FEE separately with a hot air gun. Integration time was 3000 ms.

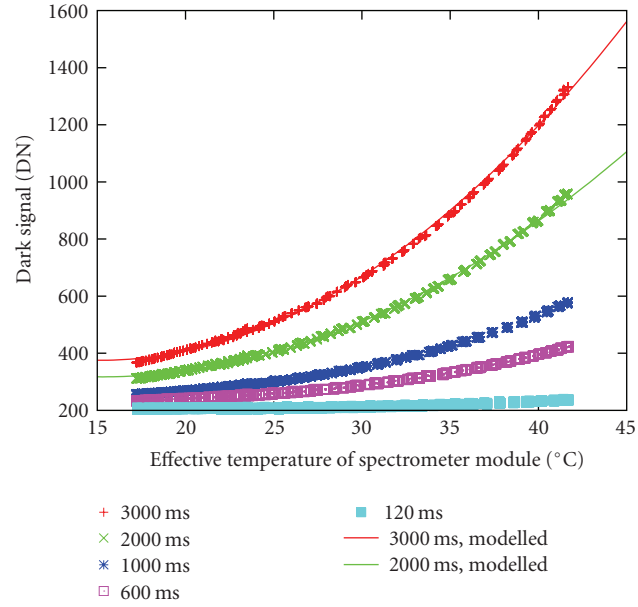

Figure 3: Dark signal temperature dependence of band no. 150 of MMS-1 at different integration times.

between dark signal and temperature is almost linear and correlation is negative. At longer integration times, the dark signal has minimal value at approximately 30°C and increases at lower and higher temperatures. It is also interesting to see that dark signal offset is negative in case of FEE-1M. The offset is adjustable but the range is too small for bringing the dark signal to positive values.

When the ambient temperature was increased from 12°C to 41°C, the thermistor voltage measured from PELTIER-tc increased from 99.7 mV to 101.5 mV which corresponds

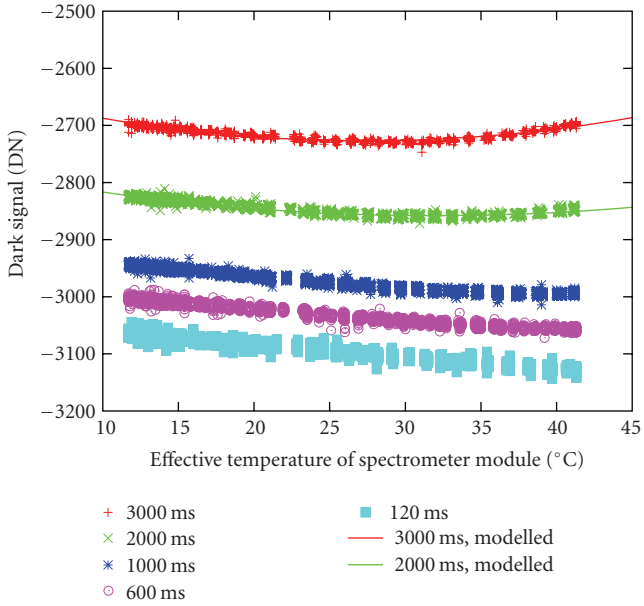

Figure 4: Dark signal temperature dependence of band no. 150 of NIR-PGS-1.7 at different integration times.

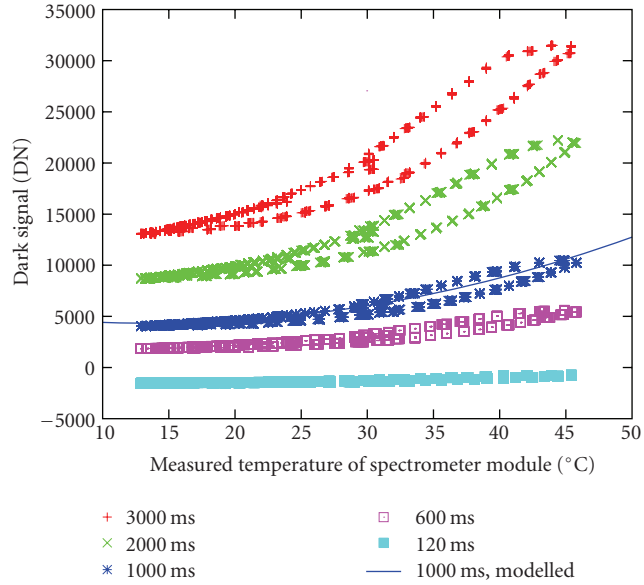

Figure 5: Dark signal temperature dependence of band no. 150 of NIR-PGS-2.2 at different integration times.

to the decrease of sensor temperature from 6.99°C to 6.55°C [16]. At the same time, setpoint voltage increased from 95.6 mV to 97.2 mV and Peltier current increased from 35 mA to 780 mA. The correlation between ambient temperature and sensor temperature was roughly linear but had hysteresis.

The dark signal temperature dependence of NIR-PGS-2.2 is plotted in Figure 5, but instead of effective temperature, the actual measured temperature is used. Although the sensor is thermoelectrically cooled down to constant temperature of −10°C [16], the dark signal depends very strongly on ambient temperature. The temperature dependence of the dark signal resembles that of MMS-1 but is more than one order of a magnitude stronger.

3.2. Dark Signal Response Time Compared to Temperature Change. In Figure 2, a time delay between temperature change and dark signal change is visible. The reason is that the thermistor did not directly measure the sensor array temperature but was attached to the body of the MMS-1 module. For correcting temperature-induced dark signal change, the relationship between the measured temperature and the effective sensor temperature that is related to dark signal change must first be determined.

The dark signal temperature dependence measurements were carried out simultaneously with changing the temperature. If the recorded dark signal is plotted against measured ambient temperature, a hysteresis can be seen as in Figure 5. This is caused by the propagation time of the heat from outside of the spectrometer module to the sensor. During warmup, the effective temperature is lower than the measured temperature, and during cooldown, the effective temperature is higher than the measured temperature. If we assume that dark signal change during the measurements in the refrigerator is caused only by temperature dependence, we can use the data recorded in the refrigerator experiment for estimating a relation between the measured temperature and effective temperature.

The effective temperature T_e can be modelled with the following function:

$$T_{e,i} = T_{e,i-1} + k(T_{i-1} - T_{e,i-1}), \tag{2}$$

where T is the measured temperature in °C, k is an estimated parameter, and $i = 2, 3, \ldots, N$ is the index denoting temperature measurements. It is assumed that $T_{e,1} = T_1$. First, temperature measurements were resampled at 1-second intervals in order to avoid any dependence between parameter k and the sampling interval of the original temperature measurements. Then, effective temperatures, T_e, were calculated and interpolated to the time of every dark signal measurement. Next, the exponential function

$$d_f(T_e) = p + q\exp(rT_e) \tag{3}$$

was fitted to measured dark signal where p, q, and r are fitted parameters. Finally, parameter k was estimated by minimizing the sum

$$m = \sum_{i=1}^{N}\left[d_i - d_f(T_{e,i})\right]^2, \tag{4}$$

where d is the measured dark signal and N is the number of recorded spectra.

For MMS-1, $k = 0.0054$. In Figure 2, both the measured temperature and the modelled effective temperature can be seen. The model introduces a time delay and also smooths sharp peaks in the measured temperature signal.

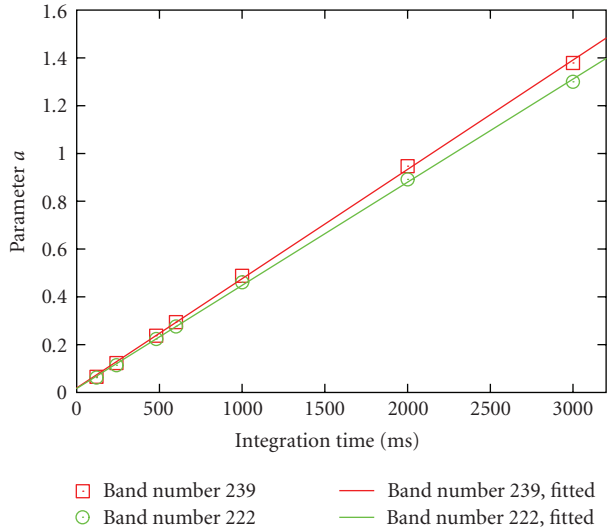

Figure 6: Parameters a_{222t} and a_{239t} for MMS-1 (see (6)).

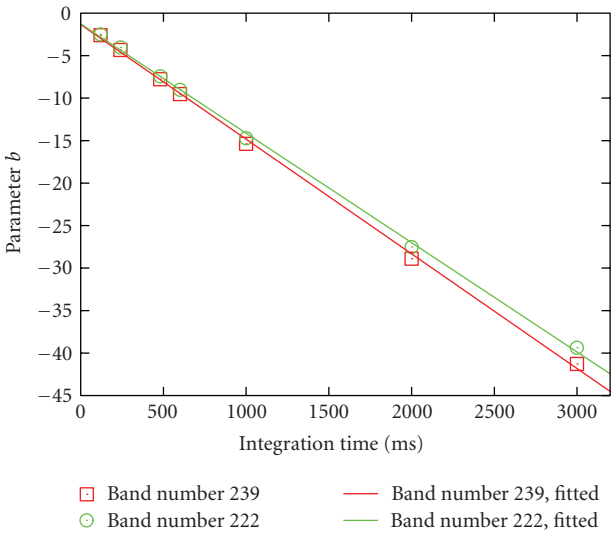

Figure 7: Parameters b_{222t} and b_{239t} for MMS-1 (see (6)).

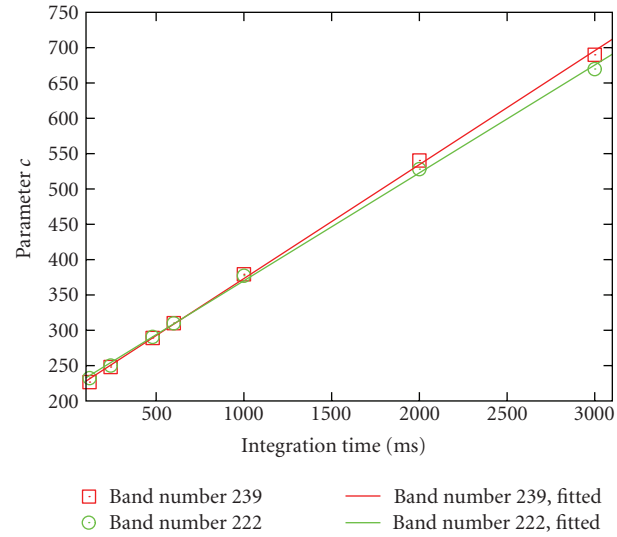

Figure 8: Parameters c_{222t} and c_{239t} for MMS-1 (see (6)).

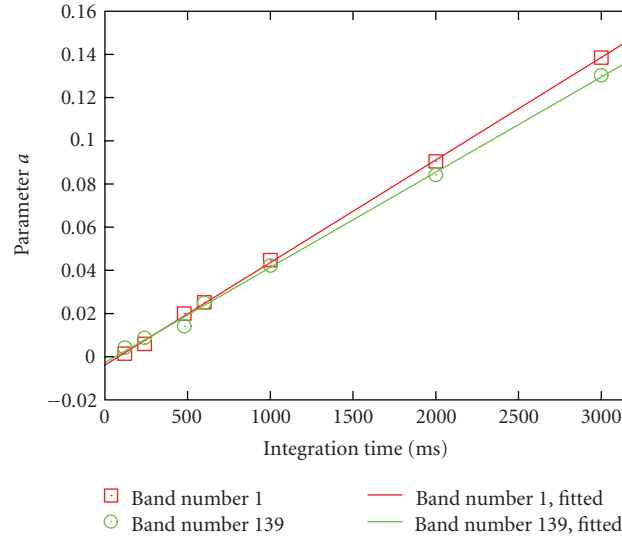

Figure 9: Parameters a_{1t} and a_{139t} for NIR-PGS-1.7 (see (6)).

In the case of NIR-PGS-1.7, there was virtually no time delay between the change of the measured temperature and spectrometer signal. Therefore, $k = 1$ can be used in (2) and the effective temperature can be expressed as

$$T_{e,i} = T_{i-1}. \tag{5}$$

This allows to use similar data processing toolchain for all the spectrometers.

For NIR-PGS-2.2, $k = 0.0025$.

3.3. Correction Algorithm. After calculation of effective temperature for each measured spectrum, dark signal temperature dependence can be corrected. For this, dark signal was measured at seven different integration times while varying ambient temperature.

The second order polynomial function

$$f_{it}(T_e) = a_{it}T_e^2 + b_{it}T_e + c_{it} \tag{6}$$

was fitted to every band at every integration time. Here, a_{it}, b_{it}, and c_{it} are fitted parameters, t is integration time, and i is band number. As parameters a_{it}, b_{it}, and c_{it} are linearly related to integration time (see Figures 6, 7, 8, 9, 10, and 11), (6) can be rewritten as follows:

$$f_i(T_e, t) = a_i(t)T_e^2 + b_i(t)T_e + c_i(t), \tag{7}$$

where

$$\begin{aligned} a_i(t) &= z_{1i}t + z_{2i}, \\ b_i(t) &= z_{3i}t + z_{4i}, \\ c_i(t) &= z_{5i}t + z_{6i}. \end{aligned} \tag{8}$$

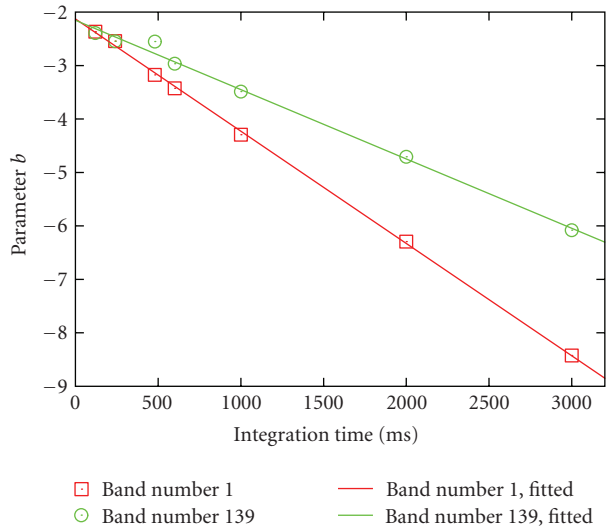

Figure 10: Parameters b_{1t} and b_{139t} for NIR-PGS-1.7 (see (6)).

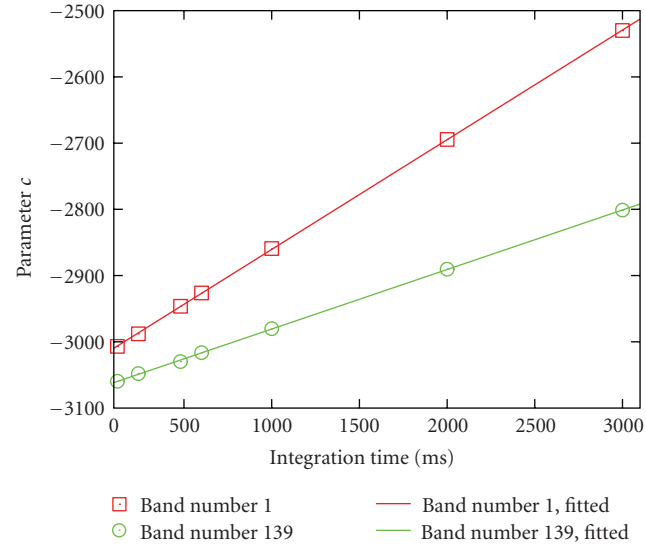

Figure 11: Parameters c_{1t} and c_{139t} for NIR-PGS-1.7 (see (6)).

If we know fitted parameters z_{ji}, $j = 1, 2, \ldots, 6$, then we can calculate dark signal $f_i(T_e, t)$ for given effective sensor temperature, T_e, integration time t, and band number i.

The agreement between modelled and measured dark signal for MMS-1 can be seen in Figure 3, where $f_{150}(T_e, 2000\,\text{ms})$ and $f_{150}(T_e, 3000\,\text{ms})$ are displayed. The same information for NIR-PGS-1.7 can be seen in Figure 4. For NIR-PGS-2.2, $f_{150}(T, 1000\,\text{ms})$ is shown in Figure 5.

Integration time and sensor temperature are not the only parameters affecting dark signal. It can depend on other factors as well, for example, long-term deterioration of electronic components. Therefore, during each measurement campaign actual dark signal measurement d_{i,T_{0e},t_0} should be used as a reference for finding dark signal $d_i(T_e, t)$ at another temperature T_e and/or integration time t

$$d_i(T_e, t) = d_{i,T_{0e},t_0} + f_i(T_e, t) - f_i(T_{0e}, t_0), \tag{9}$$

where T_{0e} and t_0 are effective sensor temperature and integration time, respectively, during reference dark signal measurement.

3.4. Validation of the Correction Algorithm. To test the correction algorithm in field conditions, an airborne measurement with closed input apertures was made for MMS-1 and NIR-PGS-1.7 spectrometer modules. After the subtraction of the dark signal, the remaining target signal should be 0, since there was no optical radiation incident on the detectors. UAVSpec2 and UAVSpec4SWIR were mounted to the frame of a Robinson R22 helicopter during a 40-minute flight. The integration times were 150 ms and 100 ms for MMS-1 and NIR-PGS-1.7, respectively. The weather conditions during the test flight were similar to those during actual field spectroscopic measurements. When the helicopter was on the ground, the sun warmed the instruments. After takeoff, the air flow generated by the main rotor and flight airspeed cooled the instruments and temperature decreased rapidly several degrees, dropping more than one degree in a minute.

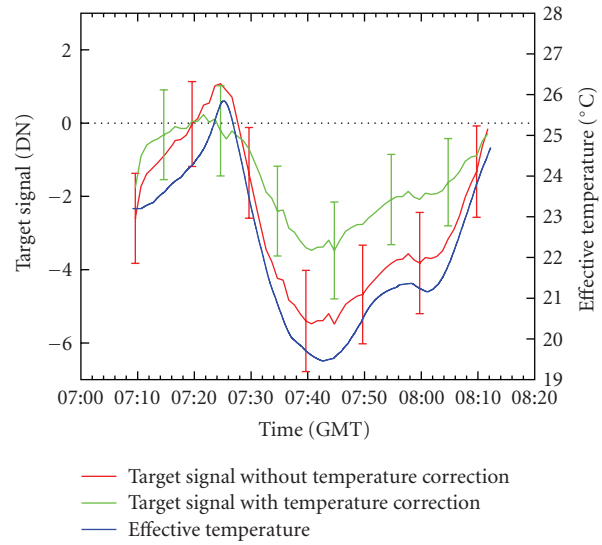

Figure 12: Validation of dark signal temperature dependence correction algorithm for MMS-1.

During flight, temperature changed a few degrees depending on flight speed, altitude, and the helicopter position relative to the Sun. After landing, the temperature of the instruments started to increase again due to the stop of the air flow and warmth of the sun.

The results can be seen in Figures 12 and 13. The helicopter took off at 07:23:40 GMT and landed at 08:01:50 GMT. The average of 100 dark signal readings recorded 3 minutes before takeoff was used as a reference dark signal d_{i,T_{0e},t_0} for the correction algorithm. T_{0e} was the average of effective temperatures during the reference dark signal measurement. Although in case of the test flight, the reference dark signal could have been chosen from any part of the measurement, this choice was made because it resembles an actual situation during field measurements—input apertures

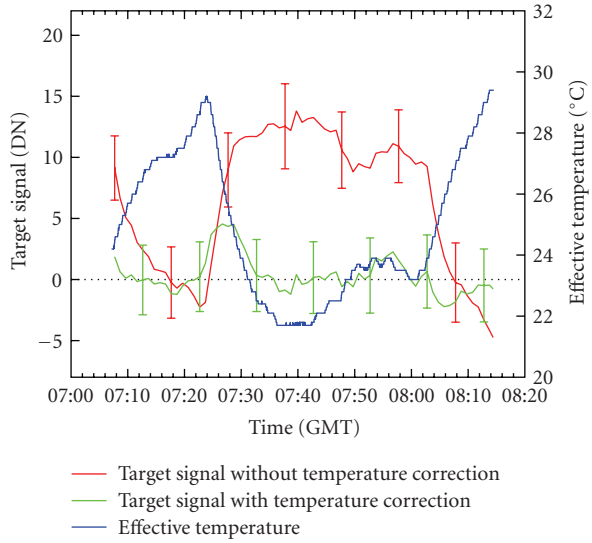

Figure 13: Validation of dark signal temperature dependence correction algorithm for NIR-PGS-1.7.

of the spectrometers cannot be closed during the flight and dark signal measurement after the flight may not be available if the battery runs out before the landing. The performance of the correction algorithm is compared to the commonly used procedure when the reference dark signal is simply subtracted from all the spectral measurements. For clarity of figures, moving averages of a single band of the target signals are shown in Figures 12 and 13. Error bars denote the standard deviation of the signal. Averaging window size is one minute.

The use of correction algorithm improved the results for both spectrometers. For MMS-1, the root mean square error (RMSE) of the target signal during the time of flight decreased 36%. In case of NIR-PGS-1.7, RMSE of the target signal decreased 68%.

Due to lack of field data, the algorithm was not validated in field conditions for NIR-PGS-2.2. However, the modelled dark signal agrees well with the data measured in the refrigerator experiment, as can be seen in Figure 5.

4. Discussion

Although the physical model of dark current temperature dependence of an uncooled junction-based detector can be described with an exponential function, a second-order polynomial function was used instead. In a limited temperature range, the polynomial function is accurate enough. The coefficients of polynomial terms are linearly related to integration time and are not very sensitive to small fitting errors. In case of the exponential function, the dependence of coefficients on integration time is more complex and even a small change in the exponential terms coefficients causes a significant change in the result.

The dark signal temperature dependence of MMS-1 and NIR-PGS-1.7 are very different. The reason is that NIR-PGS-1.7 has an InGaAs detector array which is thermoelectrically cooled and kept at a constant temperature. Nevertheless, there is still some correlation between the temperature and dark signal. When ambient temperature is increased, the setpoint voltage of PELTIER-tc also increases which causes the slight decrease of sensor array temperature. This may be caused by the increased Peltier current which warms the PELTIER-tc module. When the module is heated with a hot air gun, setpoint voltage also increases. However, this cannot be the cause of the temperature dependence visible in Figure 4. The correlation between measured sensor array temperature and calculated effective sensor temperature is linear, hence, considering the correlation between effective temperature and dark signal (see Figure 4), the correlation between measured sensor temperature and dark signal does not follow the typical exponential curve. Furthermore, the correlation between measured sensor array temperature and dark signal has significant hysteresis. Since the thermistor is inside the linear array and measures the actual temperature of the sensor, the dark signal change cannot be caused by the change of sensor temperature, but rather by the temperature sensitivity of the preamplifier circuit which is not thermally stabilized.

Despite having a thermally stabilized detector, NIR-PGS-2.2 has a very strong dark signal temperature dependence. One possible explanation to this is that in addition to dark current, thermal background may become more predominant at longer wavelengths. Only the sensor chip is cooled, but it is still sensitive to thermal radiation from surrounding mechanics [17]. Due to very strong dark signal temperature dependence, this spectrometer module should not be utilized in a setup used in UAVSpec series spectrometer systems. For obtaining reliable measurement results from this spectrometer, frequent dark signal measurements should be made, which require mechanical shutter. Another option is thermal stabilization of the whole spectrometer module, which makes the system large and increases energy consumption. However, the method described in this paper works also with this spectrometer module and improves the measurement accuracy if the previously mentioned requirements cannot be fulfilled.

The sensor temperatures in Figures 3 and 4 are effective temperatures that were calculated using the method described in Section 3.2. Although effective temperatures were modelled for PGS-NIR 2.2 as well, the temperatures in Figure 5 are those recorded simultaneously with the dark signal. This explains the strong hysteresis and also illustrates the necessity of modelling effective sensor temperatures for proper correction of dark signal temperature dependence.

It is clear from (2) that parameter k depends on the sampling interval of the temperature measurements. This means that the same sampling interval, for example, 1 second, must be used during the estimation of parameter k as well as for modelling effective temperatures for spectral measurements. Then, the effective temperatures must be interpolated to the times of spectral acquisitions for modelling separate dark signal values for each spectrum.

Parameter k also depends on the location and properties of the temperature sensor. Every time the temperature sensor is removed, k must be re-estimated. If the temperature sensor

has short response time and is exposed to surrounding air, it records the temperature change before it reaches the sensor and causes dark signal change. In case of NIR-PGS-1.7, there was virtually no time delay between the change of recorded temperature and dark signal. As previously mentioned, the temperature dependence of this spectrometer is not caused by the sensor, but rather by some of the surrounding electronics. They are smaller and more exposed to surrounding air; hence, they respond faster to temperature changes.

If the same integration time is used for target and dark signal measurements, $t = t_0$, then $c_i(t) = c_i(t_0)$ and only the first two terms of (7) remain in (9). This eliminates the error induced by fitting a linear function to parameter c_i. Therefore, if possible, the same integration time should be used for target and dark signal measurements.

A linear detector array consists of several independent detectors. The dark signal of each detector should be dealt with independently. The need for an individual set of correction coefficients for each band should be evident when looking at Figures 6–11, where the parameters a_{it}, b_{it}, and c_{it} of two different bands can be seen. The difference between bands is not very significant for silicon sensors, but very big in the case of InGaAs detectors.

Figures 12 and 13 reveal that due to several reasons the correction algorithm does not entirely remove all the errors. Not all of the dark signal change is caused by temperature dependence, but various other factors affect it as well, for example, humidity, drifts in electronic circuits, and so forth. Even after the correction some correlation between effective temperature and target signal is visible in Figure 12. This can be caused by errors introduced during parametrization of dark signal temperature dependence or even by the change of the dependence itself between laboratory measurements and field experiment. Nevertheless, the correction algorithm improves measurement accuracy. It should be kept in mind that the validation was done at very short integration times which correspond to the lowest series of points in Figures 3 and 4. In the case of MMS-1 the impact of the correction increases at higher temperatures and longer integration times where the dark signal temperature dependence is stronger. While the increase of temperature from 20°C to 25°C at integration time of 100 ms causes the dark signal increase of about 1 digital number (DN), the 30°C to 35°C temperature change at integration time of 3000 ms increases dark signal by 235 DN.

The measured target signal may have high dynamic range. The signal reflected from green vegetation under natural illumination conditions measured with MMS-1 has about 100 times difference between 350 nm and 750 nm bands. If signal at 750 nm band is 20000 DN, then dark signal error of 10 DN is insignificant for this band, but at the same time it is already 5% of the signal at 350 nm band.

Integration time and temperature are the two factors that have the strongest effect on the dark signal of a spectrometer. Integration time is always known, but it is not necessarily the same for all the measurements. Miniature spectrometer modules with uncooled sensor arrays do not have an internal thermistor for measuring the temperature of the sensor array. The spectrometers with cooled sensor arrays have a thermistor inside the sensor which is used for controlling the Peltier current. In this case, the dark signal temperature dependence is not caused by the sensor but can still be significant and should be taken into account, especially for long wavelength-type InGaAs sensors. External temperature sensor should be added to the spectrometer module and temperature should be recorded during the measurements. The temperature dependence correction method for miniature spectrometer modules described in this paper makes it possible to estimate dark signal at any temperature and integration time within reasonable range. Only six parameters for each band and one temperature modelling parameter common to all bands are needed. In field conditions, it is not always possible to take frequent dark signal readings during spectral measurements. If temperature is recorded during the measurement, this method can be used for estimating dark signal for every single spectral measurement.

Acknowledgments

This study was supported by research Grants nos. 7725 and 6812 from the Estonian Science Foundation. The author would like to thank Raul Kangro and Helina Kitsing for discussion on the modelling of effective temperatures. Valuable comments by Andres Kuusk and Jan Pisek are greatly appreciated.

References

[1] P. Berzaghi, L. Serva, and J. C. Ferlito, "Continuous analysis of grain by near infrared transmission on combines," in *Proceedings of the 9th International Conference on Precision Agriculture*, Colorado State University, July 2008.

[2] A. Larsolle, "Instantaneous measurement of reflectance spectra in the open field using diode array spectrometers," *Biosystems Engineering*, vol. 86, no. 1, pp. 1–8, 2003.

[3] N. Abu-Khalaf and B. S. Bennedsen, "Plum-tasting using near infra-red (NIR) technology," *International Agrophysics*, vol. 16, no. 2, pp. 83–89, 2002.

[4] Y. Ozaki, W. F. McClure, and A. A. Christy, *Nearinfrared Spectroscopy in Food science and Technology*, John Wiley & Sons, Hoboken, NJ, USA, 2007.

[5] P. Martinsen, J. L. Charlier, T. Willcox, G. Warman, A. McGlone, and R. Künnemeyer, "Temperature dependence of near-infrared spectra of whole blood," *Journal of Biomedical Optics*, vol. 13, no. 3, Article ID 034016, 2008.

[6] L. N. Foner, "Artificial synesthesia via sonification: a wearable augmented sensory system," *Mobile Networks and Applications*, vol. 4, no. 1, pp. 75–81, 1999.

[7] A. Kuusk, J. Kuusk, and M. Lang, "A dataset for the validation of reflectance models," *Remote Sensing of Environment*, vol. 113, no. 5, pp. 889–892, 2009.

[8] J. Kuusk, A. Kuusk, M. Lang, and A. Kallis, "Hyperspectral reflectance of boreo-nemoral forests in a dry and normal summer," *International Journal of Remote Sensing*, vol. 31, no. 1, pp. 159–175, 2010.

[9] P. Zieger, T. Ruhtz, R. Preusker, and J. Fischer, "Dual-aureole and sun spectrometer system for airborne measurements of aerosol optical properties," *Applied Optics*, vol. 46, no. 35, pp. 8542–8552, 2007.

[10] E. L. Dereniak and D. G. Crowe, *Optical Radiation Detectors*, John Wiley & Sons, New York, NY, USA, 1984.

[11] J. Kuusk and A. Kuusk, "Autonomous lightweight airborne spectrometers for ground reflectance measurements," in *Proceedings of the 2nd Workshop on Hyperspectral Image and Signal Processing: Evolutionin Remote Sensing (WHISPERS '10)*, IEEE, June 2010.

[12] Carl Zeiss Jena GmbH, "MMS—Monolithic Miniature-Spectrometer," 2002, http://www.tec5.com/downloads/datasheets/Zeiss_modules/ZEISS__PR_MMS_engl.pdf.

[13] Tec5 AG, "Front end electronics for NMOS spectral sensors and PDAs," 2006, http://www.tec5.com/downloads/datasheets/technical%20datasheets/ds_fee-hs_e.pdf.

[14] Carl Zeiss Jena GmbH, "Plane grating spectrometer NIR-PGS 1.7. Product information," 2005, http://www.tec5.com/downloads/datasheets/Zeiss_modules/pgs-nir_1_7_e.pdf.

[15] Carl Zeiss Jena GmbH, "Plane grating spectrometer NIR-PGS 2.2. Product information," 2005, http://www.tec5.com/downloads/datasheets/Zeiss_modules/pgs-nir_2_2_e.pdf.

[16] Tec5 AG, "Temperature controller module for peltier-cooled detector arrays," 2006, http://www.tec5.com/downloads/datasheets/technical%20datasheets/ds_PELTIER-tc_e.pdf.

[17] P. Huber, OEM components product manager, Tec5AG, In der Au 27, 61440 Oberursel, Germany (personal communication, 2009).